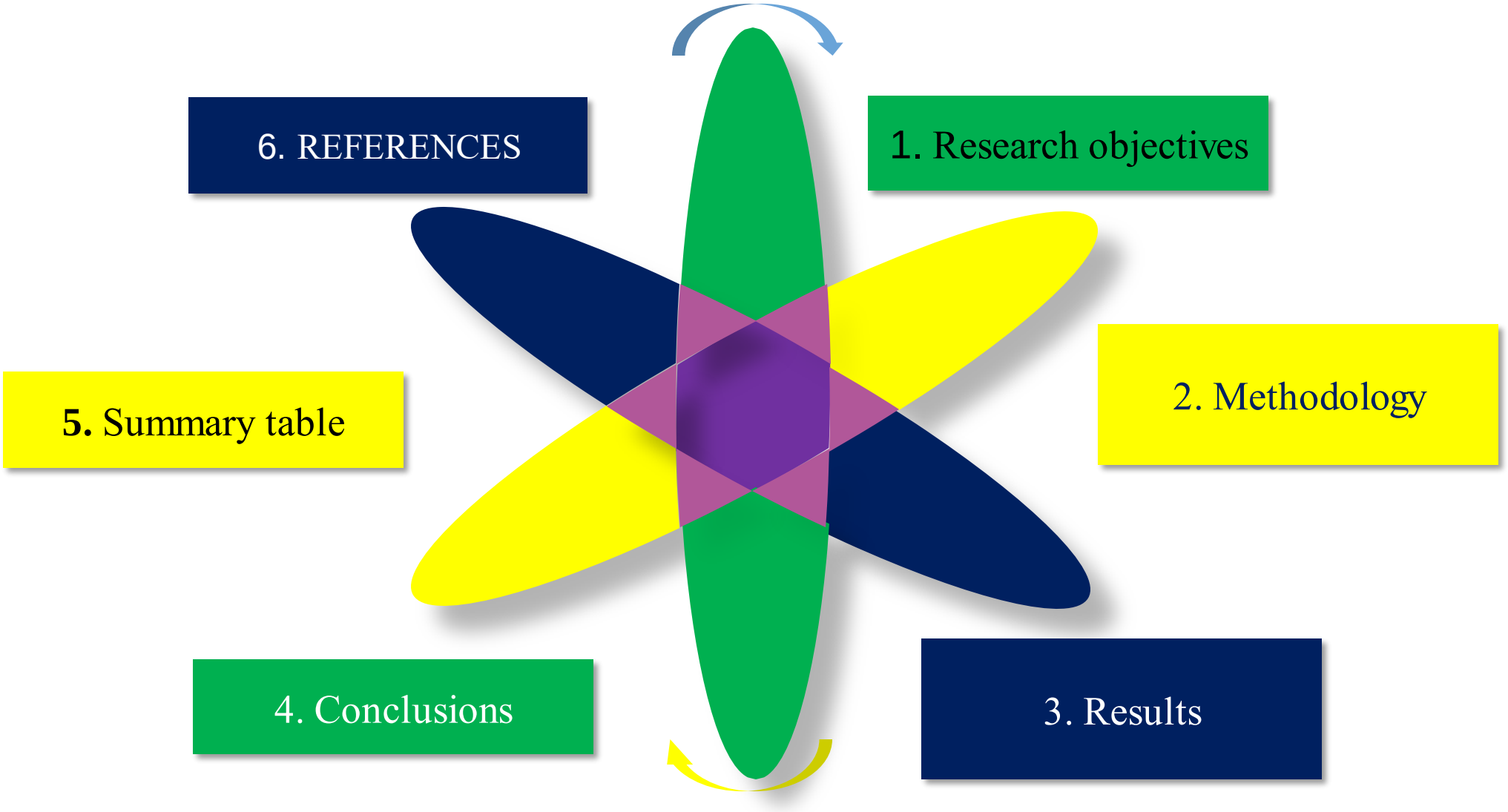
Comparative Neutronic Analysis of UO_2 and Thorium-Based $(Th,U)O_2$ MOX Cores for the APR-1400 Reactor Using a Two-Step DeCART2D/MASTER Methodology

Prepared by : Mirmakhsum Yakhyoev

November 9, 2026

CONTENTS


6. REFERENCES
1. Research objectives
5. Summary table
2. Methodology
4. Conclusions
3. Results

1. RESEARCH OBJECTIVES

GOAL

To implement **(Th,U)O_2** fuel in an initial core of APR1400 and verify its efficiency



OBJECTIVES

- ❖ to construct an initial core model of the APR-1400 loaded with UO_2 that reproduces the neutronic parameters reported in the Design Control Document (DCD),
- ❖ to compare the nuclear design parameters of UO_2 and **(Th,U)O_2** cores.

2. Methodology



Two-step reactor physics methodology:

- **DECART 2D**: performs assembly-level lattice physics and depletion calculations,
- **MASTER**: performs full-core diffusion and depletion analysis

What steps have been taken?

Step 1: Define Input Parameters
-design all fuel assemblies loaded with UO_2 fuel,
-generate cross sections for each FA,
-find out **(Th,U)O_2** fuel composition of each fuel assembly based on k_∞ values of UO_2 fuel.

Step 2: Design a core in MASTER:
-model the initial core loading pattern of APR-1400,
-verify results with DCD,
-use the same designed model for **(Th,U)O_2** MOX core.

Step 3: Compare UO_2 and MOX cores:
-calculate PPF, MTC, FTC, fast and thermal fluxes, fissile and fertile inventories, conversion ratio for UO_2 and **(Th,U)O_2** fuels .

2. Methodology
2.1 Fuel cell and fuel assembly designs

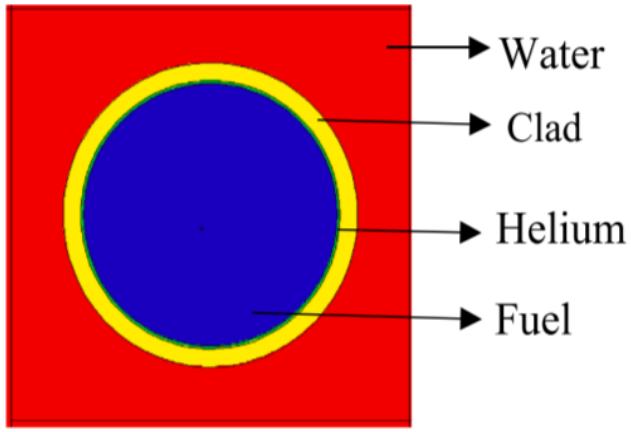


Figure 1. Horizontal layout of the fuel cell

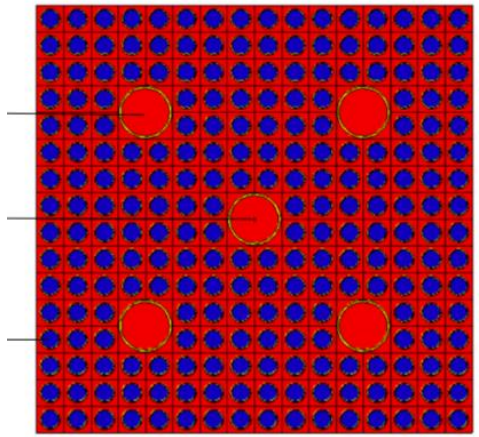


Figure 2. Horizontal layout of the fuel assembly

- 4 Guide tubes
- 1 Instrumentation tube

❖ Fuel assembly specifications and core design parameters were based on the DCD.

2. METHODOLOGY
2.2 Fuel assembly specifications of initial cycle of APR1400

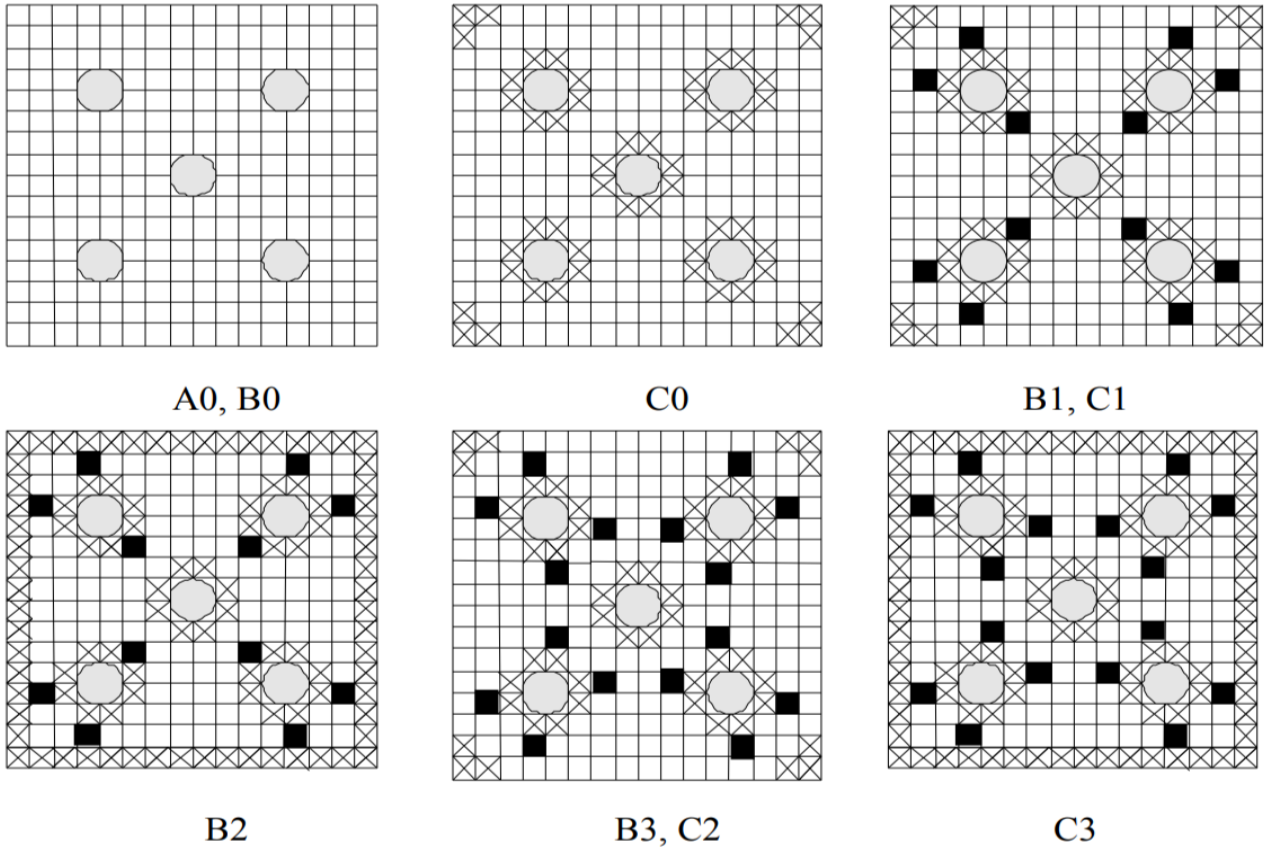


Figure 3. Fuel assembly design specifications of the APR-1400

All fuel assemblies are designed to have:

- ❖ Octant/quadrant-symmetric fuel lattice,
- ❖ Reflective boundary conditions,
- ❖ Full-power operating conditions.

- ➢ **Gd-bearing assemblies:** 12 or 16 Gd rods;
- ➢ 8 wt% Gd_2O_3.
- ➢ **MOX design:** Homogeneous fuel composition for consistent comparison with the UO_2 core.

2.METHODOLOGY
2.3 Initial core of APR 1400

Core modelling assumptions:

-all burnable absorber rods contain 2 wt% ^{235}U,

- Gd is present only in the central 92% of BA rods, excluding the top and bottom 12 inches

					C0	B0	C0	B0
			C0	C0	B2	B1	B3	C2
		C0	C1	B1	A0	C3	A0	B3
	C0	C1	B3	A0	B3	A0	B1	A0
	C0	B1	A0	C2	A0	C3	A0	B1
C0	B2	A0	B3	A0	B3	A0	B3	A0
B0	B1	C3	A0	C3	A0	C2	A0	C3
C0	B3	A0	B1	A0	B3	A0	B3	A0
B0	C2	B3	A0	B1	A0	C3	A0	A0

Figure 4. Initial core map of APR 1400

2. METHODOLOGY
2.4 $(Th,U)O_2$ fuel isotopic composition
2.4.1 $(Th,U)O_2$ fuel definition and k_∞ matching

- Fuel composition (wt%): ^{232}Th (80.9–84.4 wt%) · U (3.5–7.0 wt%) · O (12.11wt%),
- Uranium vector: 80 wt% ^{235}U + 20 wt% ^{238}U,
- U content: 4–8 wt% of heavy metal (Th + U),
- ^{232}Th fraction was determined through a parametric search, with the remaining isotope weight fractions (^{235}U, ^{238}U, ^{16}O) recalculated for each assembly,
- $(Th,U)O_2$ enrichment iteratively adjusted to match the corresponding UO_2 assembly's k_∞ ,
- Maximum k_∞ mismatch: 84 pcm.

2.METHODOLOGY
2.4 $(Th,U)O_2$ fuel isotopic composition
2.4.2 $(Th,U)O_2$ composition for all fuel assemblies

Table 1. MOX fuel isotope composition for high and low enrichments

FA type	Enrichment	^{235}U (wt%)	^{238}U (wt%)	^{16}O (wt%)	^{232}Th (wt%)
A0	High	2,82	0,70	12,11	84,37
B0	High	4,92	1,23	12,11	81,74
B1	High	4,24	1,06	12,11	82,59
	Low	3,52	0,88	12,11	83,49
B2	High	4,25	1,06	12,11	82,57
	Low	3,53	0,88	12,11	83,48
B3	High	4,15	1,04	12,11	82,71
	Low	3,30	0,83	12,11	83,76
C0	High	5,62	1,41	12,11	80,86
	Low	4,99	1,25	12,11	81,65
C1	High	4,85	1,21	12,11	81,83
	Low	4,22	1,05	12,11	82,62
C2	High	4,64	1,16	12,11	82,09
	Low	4,22	1,05	12,11	82,62
C3	High	4,71	1,18	12,11	82,00
	Low	4,08	1,02	12,11	82,79

- MOX fuel assemblies: k_∞ matched to corresponding UO_2 assemblies,
- Fissile content (^{235}U/IHM): 3.2–6.4 wt%,

2.Methodology
2.5 MTC and FTC parameters

Method: Single-parameter perturbations from the APR-1400 reference state,

Reference state: $T_{fl} = 960.95$ K, $T_{ml} = 585.35$ K, from MASTER's coupled 3-D thermal-hydraulic solution,

MTC: $\Delta T_m = 3$ K, with boron, power, and xenon fixed,

FTC: $\Delta T_f = 3$ K, under isothermal conditions,

2 Methodology
2.6 Conversion ratio

The relevant conversion ratio is

$$CR = \frac{\text{fissile material production rate}}{\text{fissile material consumption rate}}.$$

$$\mathrm{CR} = \frac{\phi\Sigma_c^{U-238} + \phi\Sigma_c^{Pu-238} + \phi\Sigma_c^{Pu-240}}{\phi\Sigma_a^{U-235} + \phi\Sigma_a^{Pu-239} + \phi\Sigma_a^{Pu-241}} \quad (1)$$

$$\mathrm{CR} = \frac{\phi\Sigma_c^{Th-232} + \phi\Sigma_c^{U-238} + +\phi\Sigma_c^{Pu-238} + \phi\Sigma_c^{Pu-240}}{\phi\Sigma_a^{U-233} + \phi\Sigma_a^{U-235} + \phi\Sigma_a^{Pu-239} + \phi\Sigma_a^{Pu-241}}$$

(2)

At the fuel assembly-level, CR values were computed for the A_0-type assembly

- **First method:** the core average enrichments are 2.66% for UO_2 and 3.48% for UO_2 and **(Th,U)O_2** .
  - The initial fertile-to-fissile atom ratio: 36.1 in the UO_2 core and 24.6 in the **(Th,U)O_2** MOX core.
- **Second method**: the same core-average enrichment of 2.66 wt% for both fuel configurations.

•**Data limitation**: the isotope-wise cross-section in the full-core depletion analysis

2 Methodology
2.6 Conversion ratio

The relevant conversion ratio is

$$CR = \frac{\text{fissile material production rate}}{\text{fissile material consumption rate}}.$$

$$CR_{uo2} = \frac{(N_{^{239}\mathrm{Pu},\,EOC} - N_{^{239}\mathrm{Pu},\,BOC}) + (N_{^{241}\mathrm{Pu},\,EOC} - N_{^{241}\mathrm{Pu},\,BOC})}{N_{\mathrm{fissile},\,BOC} - N_{\mathrm{fissile},\,EOC}}.$$

$$CR_{th} = \frac{(N_{^{233}\mathrm{U},\,EOC} - N_{^{233}\mathrm{U},\,BOC}) + (N_{^{239}\mathrm{Pu},\,EOC} - N_{^{239}\mathrm{Pu},\,BOC}) + (N_{^{241}\mathrm{Pu},\,EOC} - N_{^{241}\mathrm{Pu},\,BOC})}{N_{\mathrm{fissile},\,BOC} - N_{\mathrm{fissile},\,EOC}}$$

Using these formulas, conversion ratios were found:

CR_{uo2} =0.62, CR_{th} =0.59

- The lower CR obtained: differences in the initial isotopic inventory and neutron spectrum. The lower ^{238}U fraction in the **(Th,U)O_2** fuel limits the plutonium-production pathway, whereas the contribution from the $^{232}Th \rightarrow ^{233}U$ pathway develops more gradually with burnup.
- The higher soluble-boron concentration also changes the neutron absorption balance and may affect the conversion of ^{232}Th. Moreover, the k_∞-matching procedure equalizes assembly-level reactivity rather than core-average fissile inventory. Consequently, the UO_2 and **(Th,U)O_2** MOX cores have different initial fissile inventories and depletion rates, which affects the resulting CR comparison.

3. RESULTS

3.1 Comparison of k_∞ trends for $(Th,U)O_2$ and UO_2 fuel assemblies

3.1.1 A_0-fuel assembly

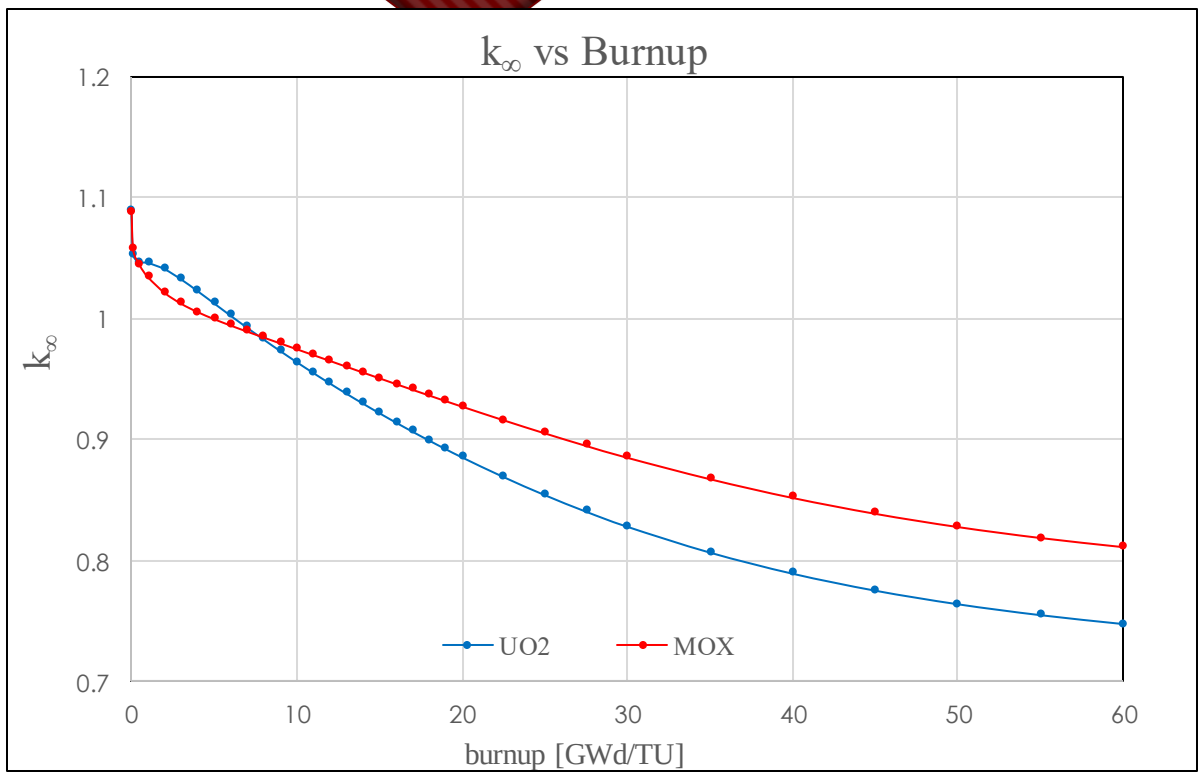


Fig. 5. k_∞ values of A_0-type fuel assembly for UO_2 and $(Th,U)O_2$ fuels

- Both UO_2 and **$(Th,U)O_2$** show a continuous decrease in k_∞ with burnup,
- **$(Th,U)O_2$** maintains a higher k_∞ than UO_2 after the initial burnup stage,
- The difference between the fuels becomes more pronounced at higher burnup.

3. RESULTS
3.1 Comparison of k_∞ trends for MOX and UO_2 fuel assemblies
3.1.2 B_2-fuel assembly

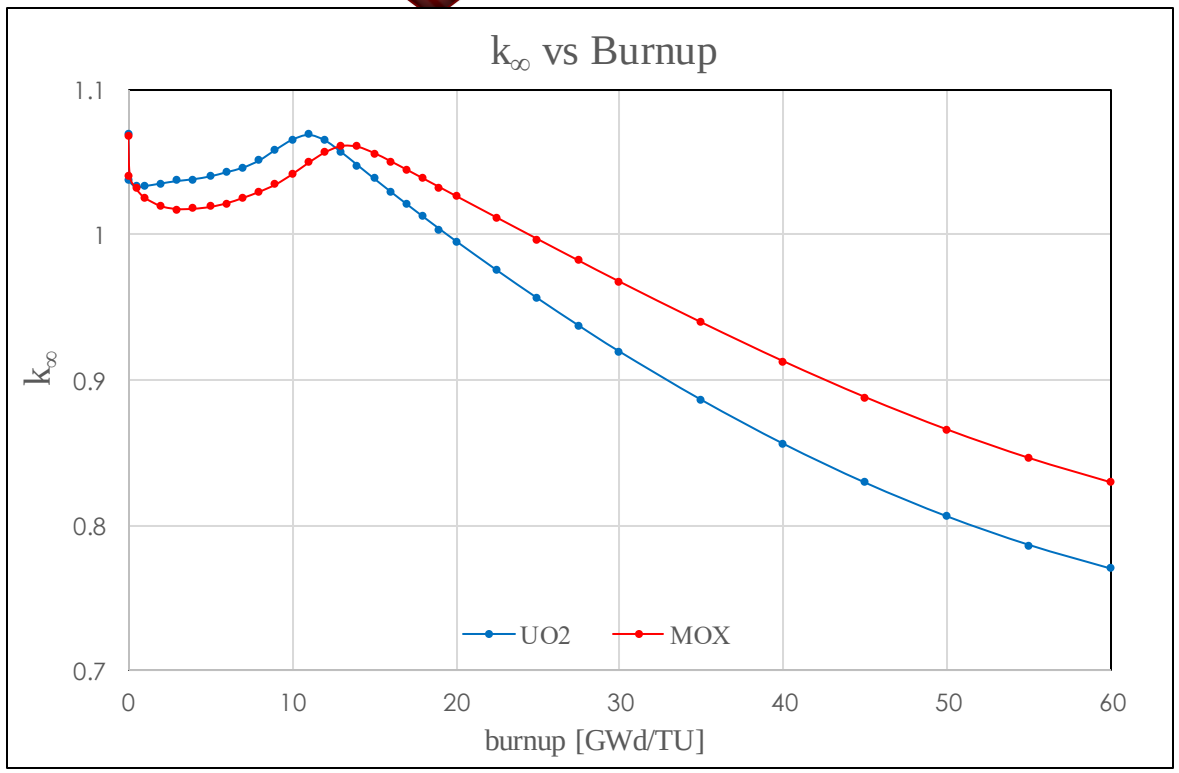


Fig. 6. k_∞ values of B_2-type fuel assembly for UO_2 and $(Th,U)O_2$ fuels

- Initial increase in k_∞ due to gadolinium depletion, followed by a continuous decline,
- $(Th,U)O_2$ maintains a higher k_∞ than UO_2 over most of the burnup range,
- The difference between the fuels widens at higher burnup.

3.RESULTS
3.2 Comparison of cycle burnup and CBC with DCD reference

Table 2. Deviation of calculated CBC (UO_2) from the DCD at selected points.

Parameter	DCD	Calc.	Deviation
CBC	[ppm]		
0 EFPD	817.00	783.98	33.02
90 EFPD	739.30	685.43	53.87
210 EFPD	682.57	622.58	59.99
450.64 EFPD	46.00	10.06	35.94

- **CBC:** Follows the DCD trend but is consistently underpredicted, with a maximum deviation of 59.99 ppm.
- **Cycle burnup:** 17.13 GWd/MTU, only 0.44 GWd/MTU below the DCD value, supporting the model's extension to the MOX case.

3. Results
3.3 $(Th,U)O_2$ - UO_2 comparison: burnup, CBC and PPF

- BOC: **$(Th,U)O_2$** MOX core requires higher CBC than UO_2 (909.10 vs 783.98 ppm) despite similar k_∞,
- Mid-cycle: **$(Th,U)O_2$** CBC falls below UO_2, reaching about 212 ppm lower near 90 EFPD,
- End-cycle: **$(Th,U)O_2$** CBC rises above UO_2, reflecting burnup-dependent changes in ^{233}U production from ^{232}Th breeding, neutron absorption, and spectrum.

Table 3. Cycle burnup and PPF values

Fuel	**UO_2**	**$(Th,U)O_2$**
Cycle burnup[GWd/T]	17.13	22.61
Cycle length [EFPD]	450.64	549.82
PPF	1.39	1.43

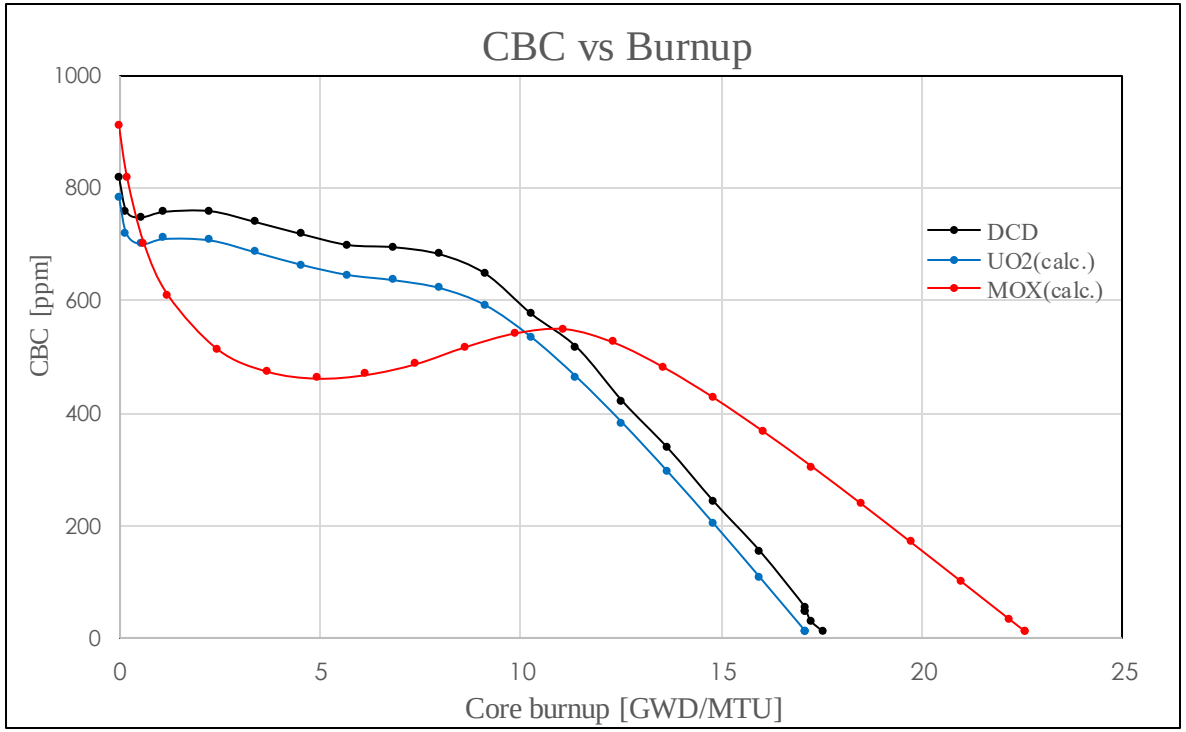


Fig. 7. CBC variation with burnup for UO_2 and $(Th,U)O_2$ fuels

3. RESULTS
3.4 Comparison of MTC

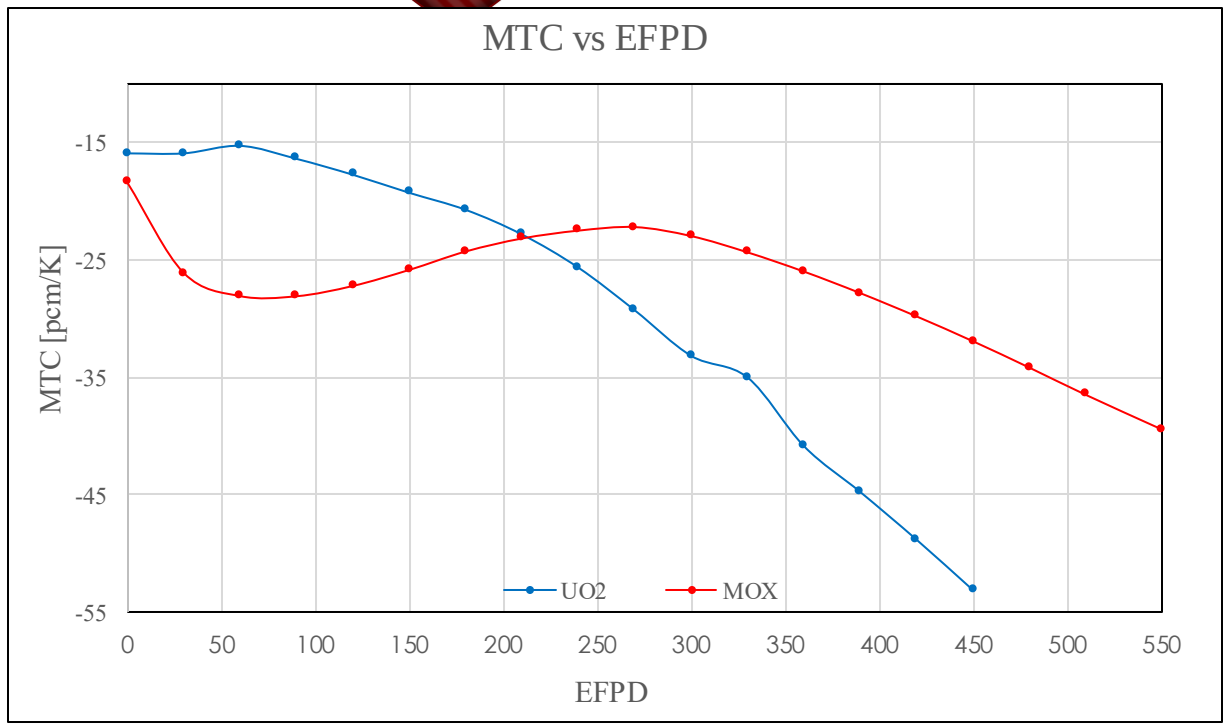


Fig. 8. MTC values for UO_2 and $(Th,U)O_2$ fuels

UO_2: Monotonic decrease from −15.92 to −53.20 pcm/K, sharper decrease,
$(Th,U)O_2$: Non-monotonic trend ranging from -18.43 to -39.45,
Both cores: Negative moderator temperature feedback throughout the cycle.

Key Insight: Different isotope inventories and neutron spectrum; altered moderation and absorption.

3. RESULTS
3.5 Comparison of FTC

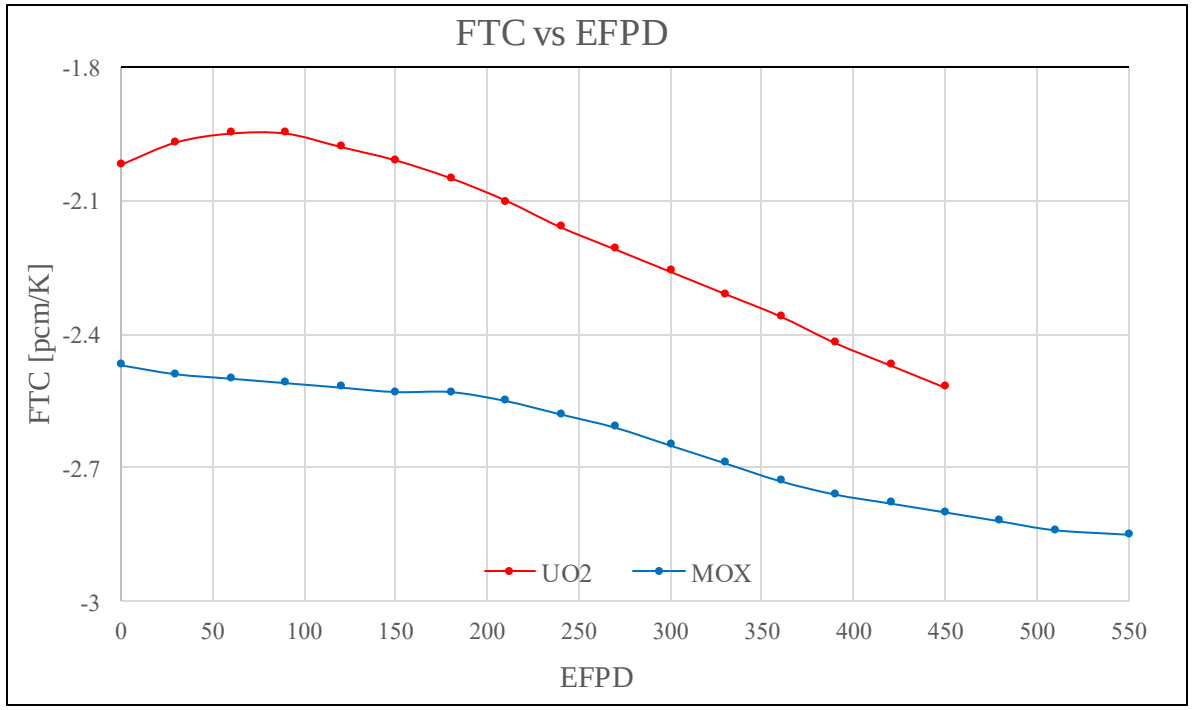


Fig. 9. FTC values for UO_2 and $(Th,U)O_2$ fuels

$(Th,U)O_2$: More negative FTC throughout the cycle (−2.47 to −2.85 pcm/K), stronger Doppler feedback in the MOX core,

UO_2: FTC ranges from −2.02 to −2.52 pcm/K,

Both cores: Negative fuel temperature feedback throughout the cycle.

Key insight: Different fertile-isotope inventories and isotopic evolution; stronger Doppler feedback in **$(Th,U)O_2$** .

3. RESULTS
3.6 Thermal Flux comparison

ϕ_{therm}, $E \leq 0.625$ eV

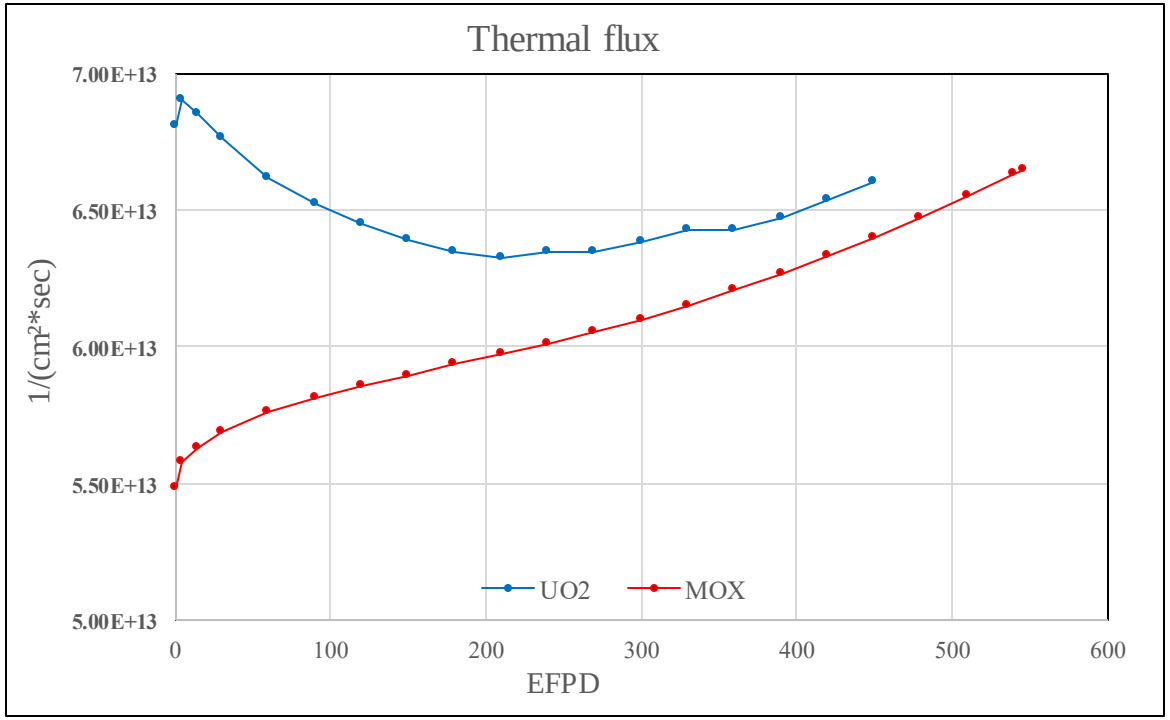


Fig.10. Thermal flux variation

- **(Th,U)O_2 :** Lower thermal flux, increasing from $5.48 \cdot 10^{13}$ to $6.65 \cdot 10^{13}$ $cm^{-2}s^{-1}$ over the cycle,
  - Evolving neutron absorption and isotope inventories during burnup, including changes associated with absorber depletion.

- **UO_2:** Initial decrease followed by recovery,
  - Changes in fuel composition, neutron absorption, and spectrum during early burnup.

3. RESULTS
3.7 Fast Flux comparison

ϕ_{fast}, E > 0.625 eV

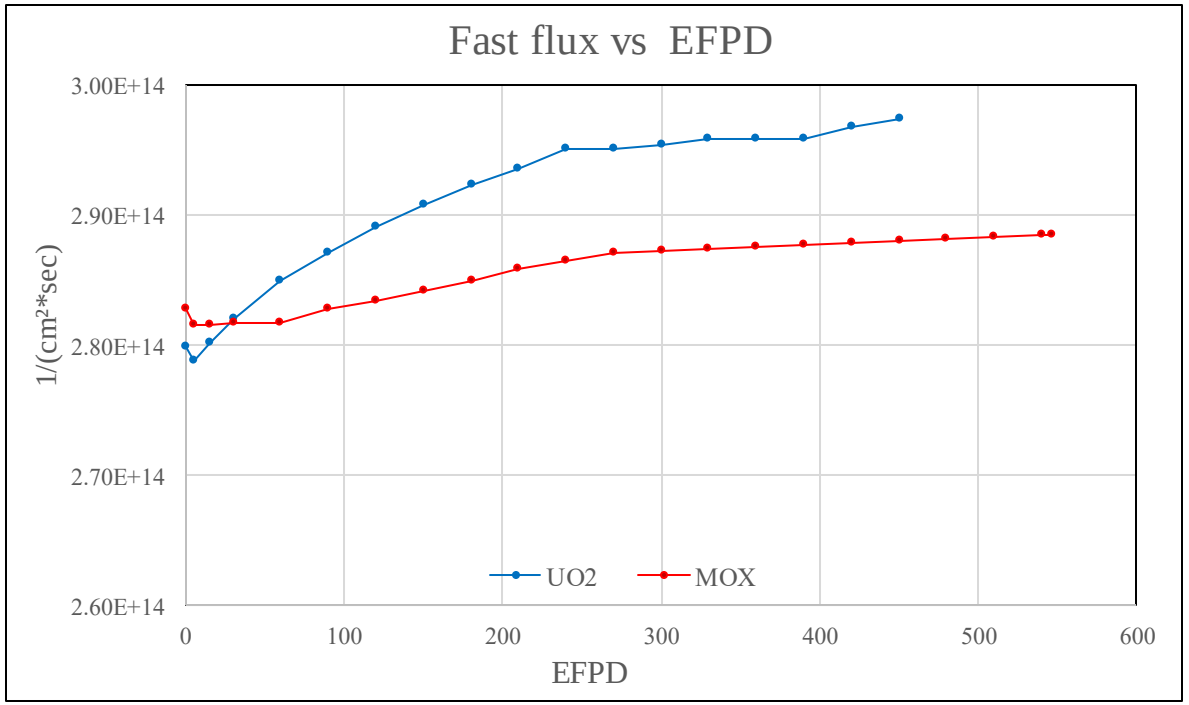


Fig.11. Fast flux variation.

UO_2 core: increases from $2.80 \cdot 10^{14}$ to $2.97 \cdot 10^{14}$ $cm^{-2}s^{-1}$,remaining higher during most of the cycle, **$(Th,U)O_2$ MOX core:** Slight initial decrease, followed by a gradual increase to around $2.89 \cdot 10^{14}$ $cm^{-2}s^{-1}$.

Key insight: Evolving fissile inventories, neutron production, and energy-dependent absorption cross sections.

3. RESULTS
3.8 Fast-to-Thermal Flux Ratio

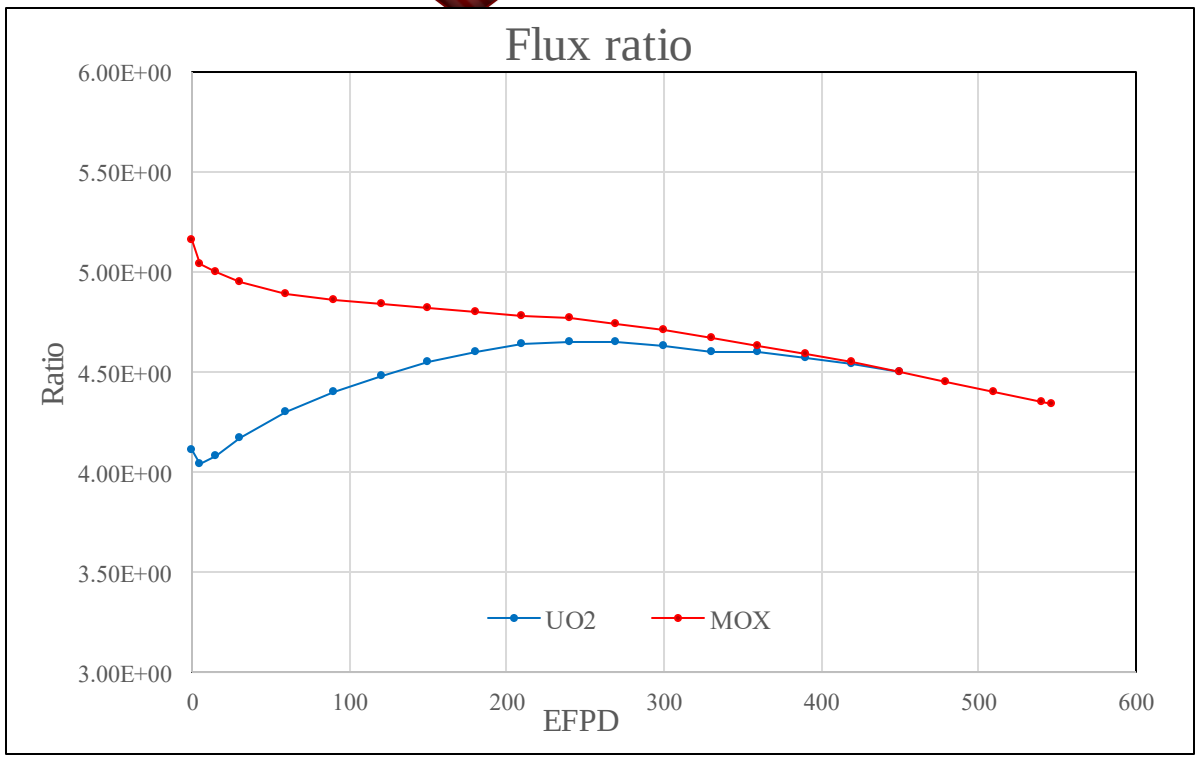


Fig.12. Flux ratio variation

- **BOC**: Higher ratio in MOX (5.22) than UO_2 (4.12),
- **EOC:** MOX converges to 4.5 while UO_2 stands at 4.35,

❖ **UO_2:** increases initially, peaks near mid-cycle, then decreases(reflects changes in the relative fast and thermal fluxes during burnup),

❖ **$(Th,U)O_2$:** decreases progressively during burnup(a reduction in fast flux relative to thermal flux),

➢ Contributing factors: Changes in neutron absorption and fuel-isotope inventories

3. RESULTS
3.9 Axial power distribution
3.9.1 Beginning of cycle

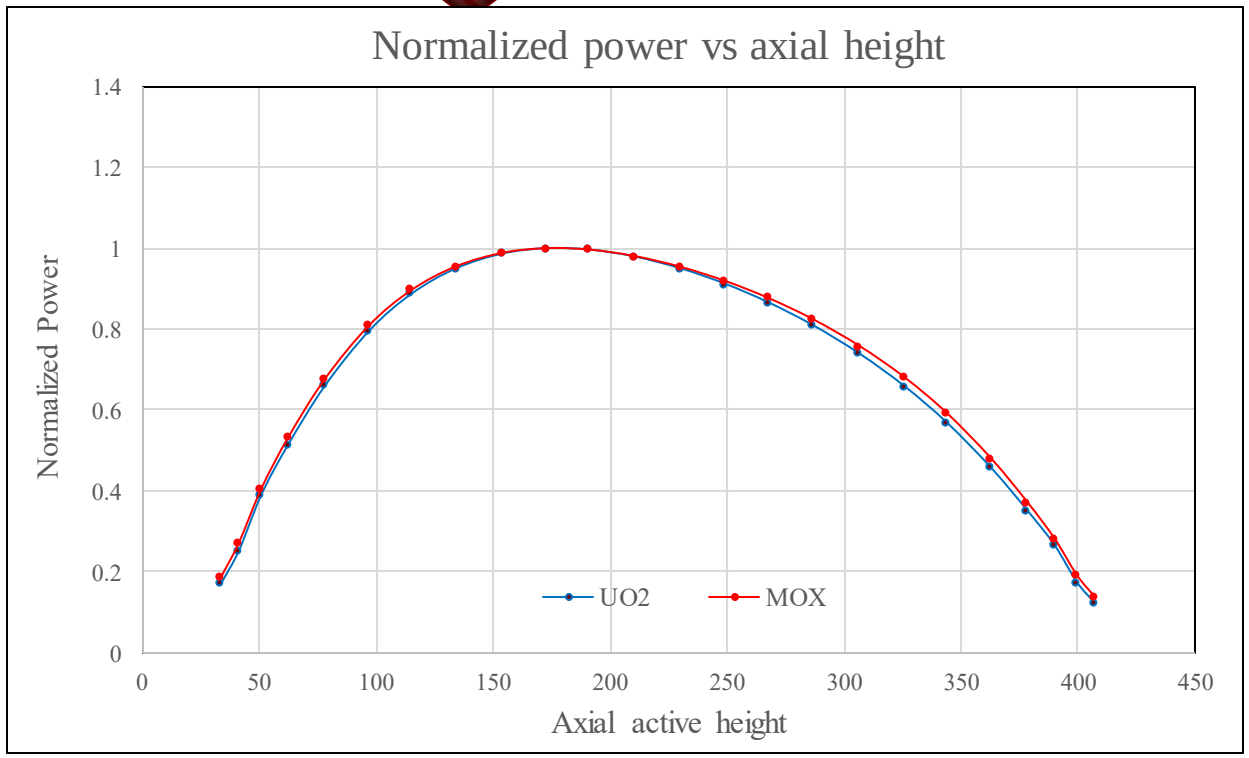


Fig. 13. Normalized power at BOC.

- **UO_2 vs $(Th,U)O_2$** : Nearly identical axial power profiles at BOC,
- **Power shape**: Central peak with lower power near the axial ends,

Contributing factors: Fresh, axially uniform fuel with minimal burnup and fissile-inventory differences along the core height.

3. RESULTS
3.9 Axial power distribution
3.9.2 End of cycle

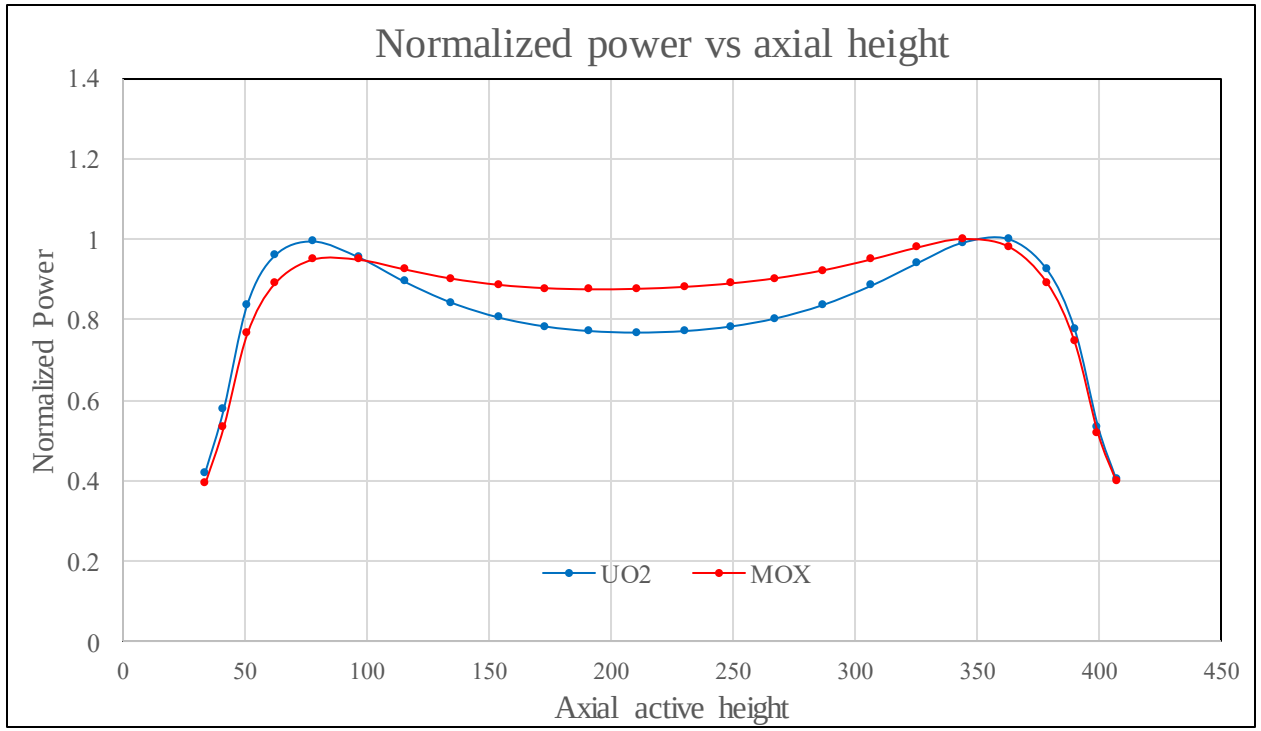


Fig. 14. Normalized power at EOC

$(Th,U)O_2$: Shallower power depression and 14% higher relative power level in the middle-to-lower core region (0.87),

UO_2: More pronounced depression (0.76).

3. RESULTS
3.10 Fertile and fissile inventories

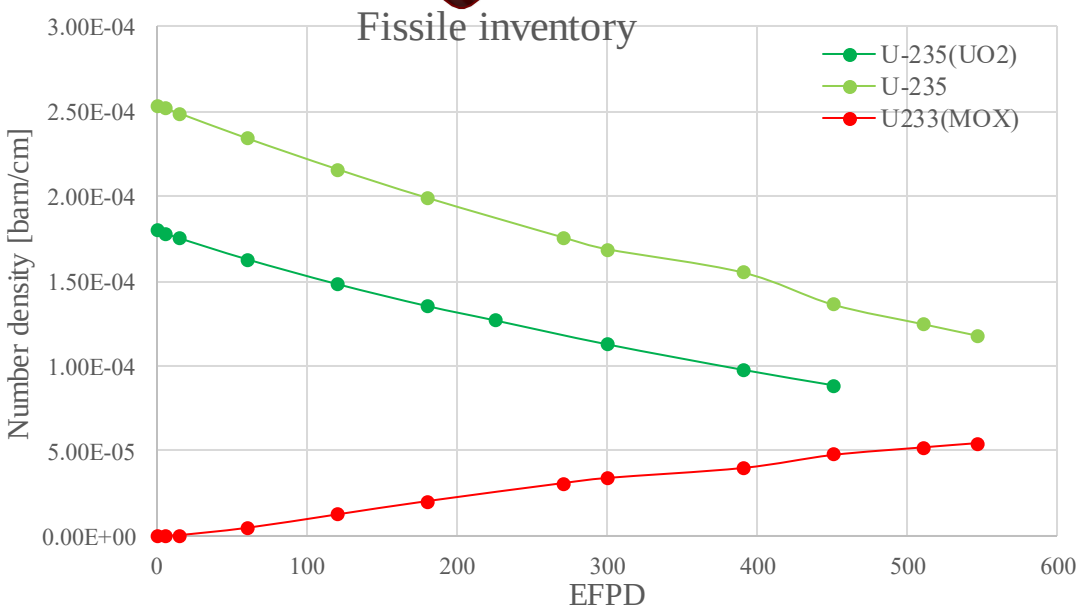


Fig. 15. Fissile inventory

UO_2: ^{235}U inventory decreases,
$(Th,U)O_2$: ^{235}U decreases,
whereas ^{233}U builds up.

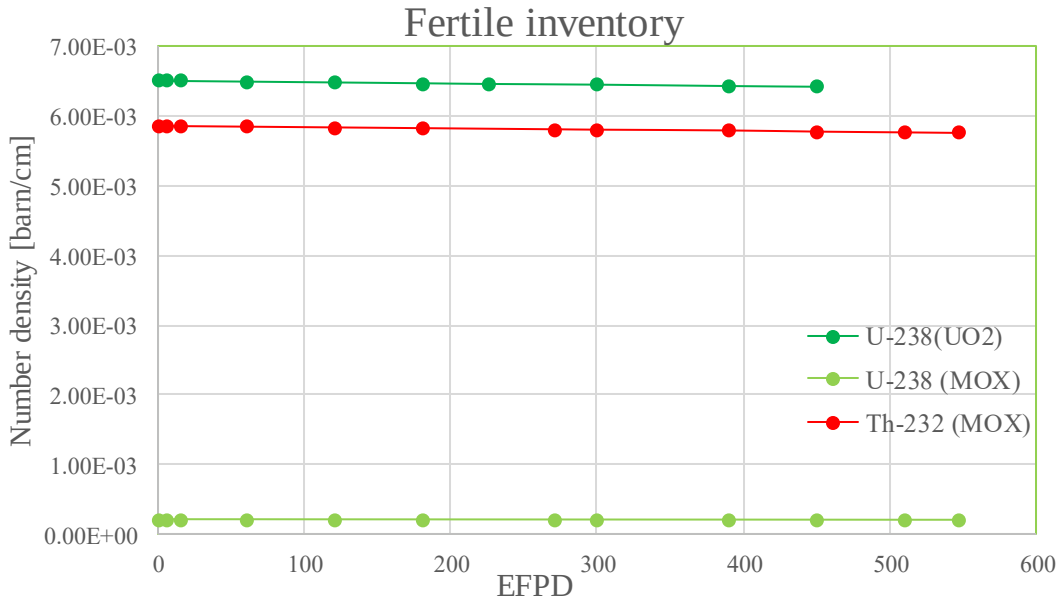


Fig. 16. Fertile inventory

UO_2: ^{238}U is the main fertile material,
$(Th,U)O_2$: ^{232}Th is the main fertile isotope, ^{238}U inventor is much smaller,
Both fuels: Fertile inventories decrease modestly, follow different fissile-production pathways

3. RESULTS.
3.11 Plutonium buildup

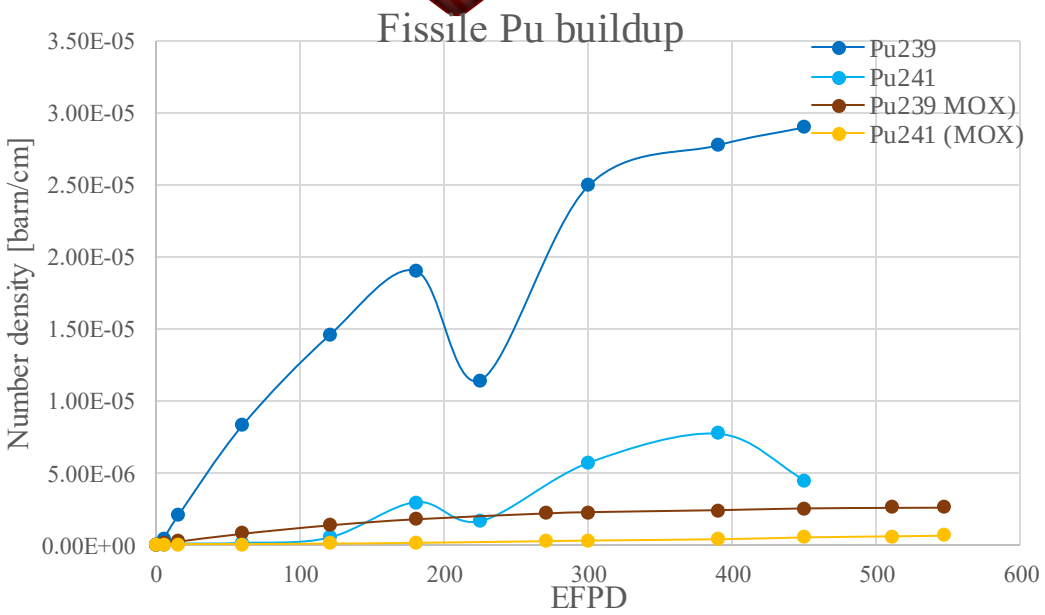


Fig. 17. Fissile Pu isotopes buildup

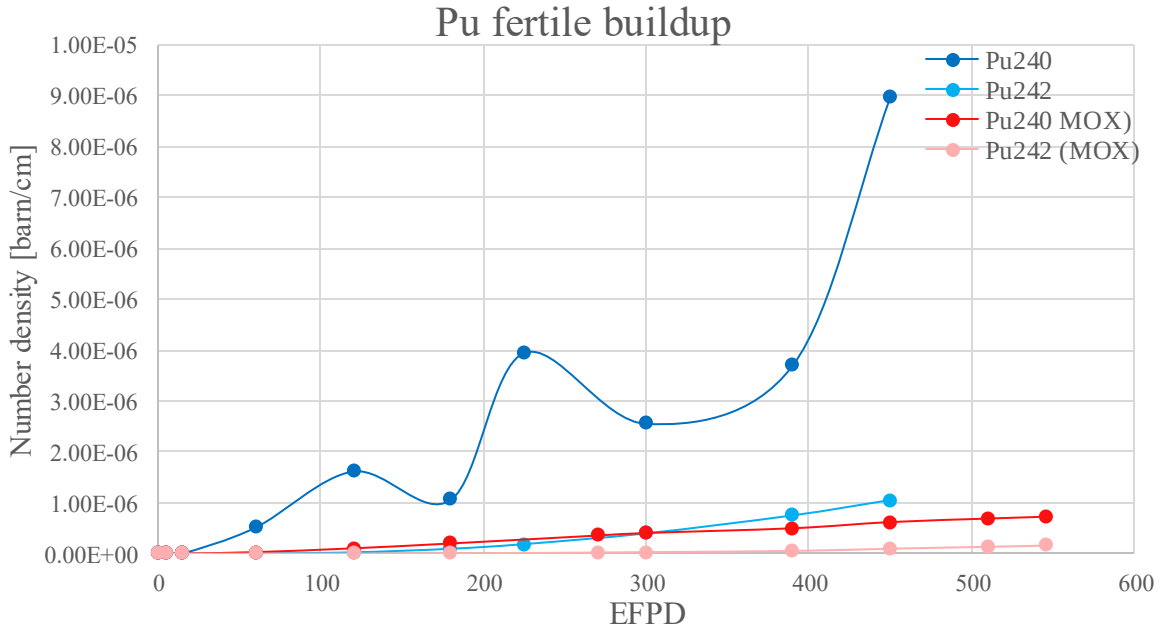


Fig. 18. Fertile Pu isotopes buildup

- **UO_2:** Substantial ^{239}Pu, ^{241}Pu also accumulates (Stronger plutonium-production pathway)
- **$(Th,U)O_2$:** Much lower concentrations of fissile plutonium isotopes

- **UO_2:** Significant neutron capture and ^{240}Pu, ^{242}Pu isotopes buildup,
- **$(Th,U)O_2$** : Lower plutonium production

3.RESULTS
3.12 Conversion ratio

Table 4. CR values

Comparison scenario	UO_2	$(Th,U)O_2$
Design-specific enrichment	2.66%; CR = 0.72	3.48%, CR=0.69
Equal enrichment		2.66%; CR = 0.79

- **Enrichment sensitivity:** The relative CR ranking reverses between the design-specific and equal-enrichment cases,
- **Key implication:** CR depends on initial fuel composition, fissile inventory, and neutron spectrum [5,6]
- **Interpretation:** CR alone is insufficient to predict cycle-length performance.

4. CONCLUSIONS

•**Methodology validation:** The DeCART2D/MASTER UO_2 model reproduced the DCD cycle burnup within 0.44 GWd/MTU, supporting its application to the **(Th,U)O_2** case.

•**Core performance: (Th,U)O_2** extended cycle length from 450.64 to 549.82 EFPD and discharge burnup from 17.13 to 22.61 GWd/MTU, with higher CBC and a slightly higher maximum PPF.

•**Reactivity feedback: (Th,U)O_2** exhibited more negative FTC and a non-monotonic MTC trend; both cores maintained negative temperature feedback throughout the evaluated cycle.

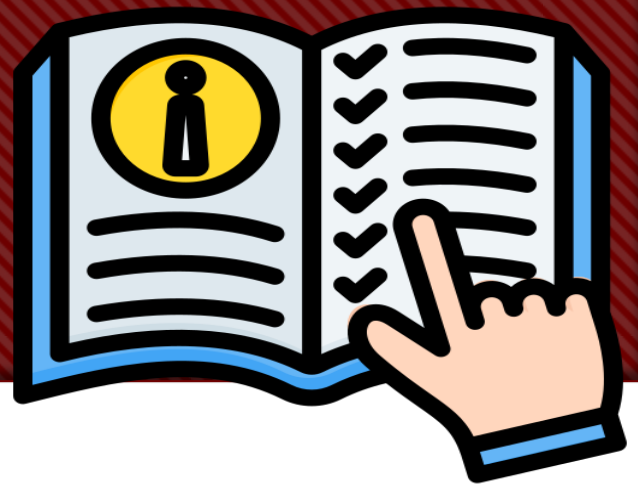
5. Summary table

Table 5 summarizes the UO_2 model validation against the DCD reference and the key performance differences between the UO_2 and **$(Th,U)O_2$** MOX cores.

Table 5. Summary table

Parameter	**DCD reference (UO_2)**	**Calculated UO_2**	**Calculated $(Th,U)O_2$**
CBC at BOC (ppm)	817	783.98	909.10
Cycle burnup (GWd/T)	17.57	17.13	22.61
Cycle length (EFPD)	—	450.64	549.82
Max PPF	—	1.39	1.43

6.REFERENCES



[1] A.A. Galahom, A.S. Khaliil, N. Alnassar, S.M. Reda, Discussing the possibility of using thorium-based fuels as an alternative fuel to uranium dioxide fuel for APR-1400 reactor, Nucl. Eng. Des. 417 (2024) 112817.

[2] Korea Hydro & Nuclear Power Co. (KHNP), APR1400 Design Control Document (DCD), KHNP, Gyeongju, Republic of Korea.

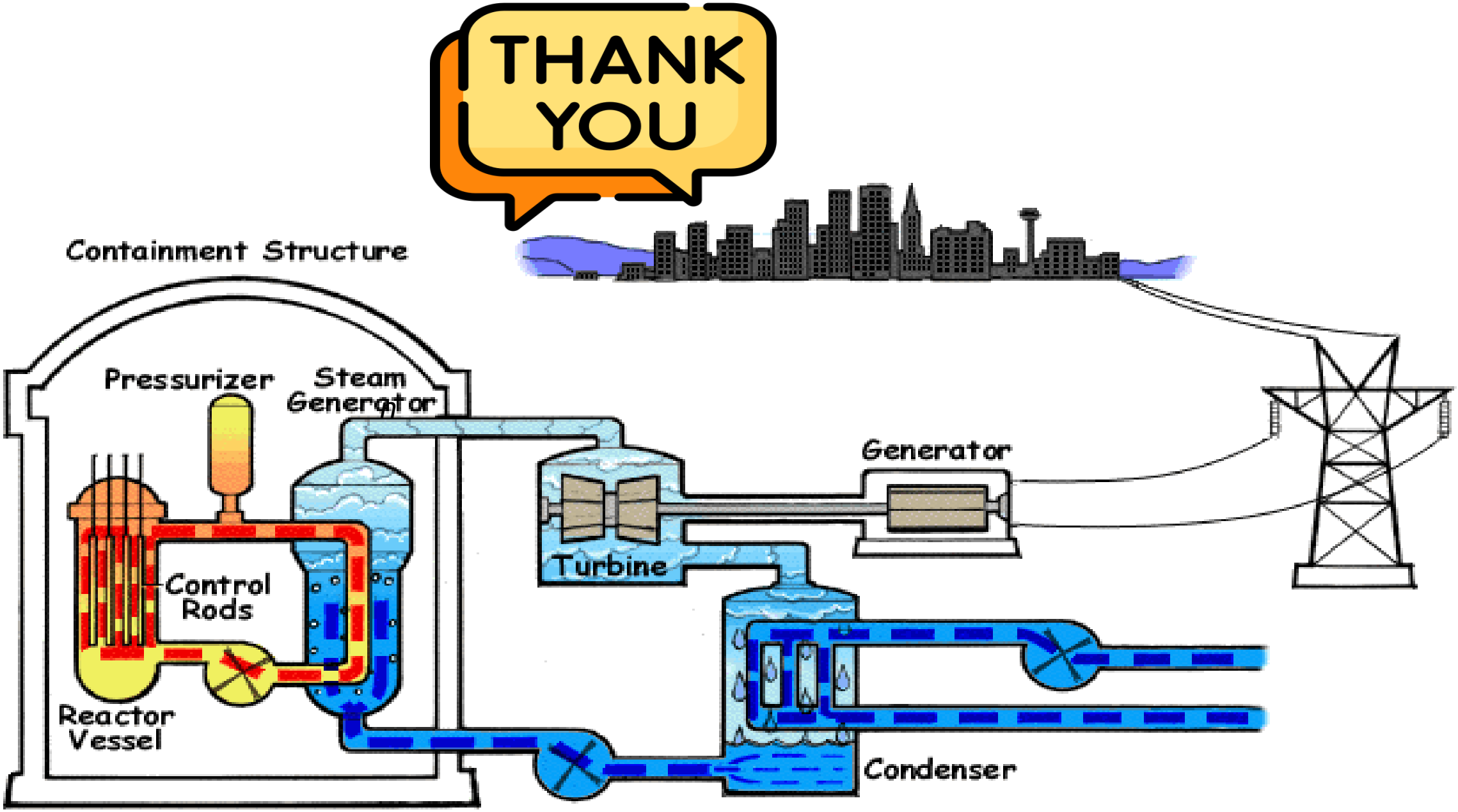
[3] Korea Atomic Energy Research Institute (KAERI), DeCART2D v1.1 User's Manual, KAERI, Daejeon, Republic of Korea.

[4] Korea Atomic Energy Research Institute (KAERI), MASTER Code User's Manual, KAERI, Daejeon, Republic of Korea.

[5] Nabila, U.M., Sahadath, M.H., Rohan, H.R.K., Potential of mixed oxide fuel for higher fissile conversion ratio in light water reactors. Nucl. Eng. Des. 424 (2024), 113295.

[6] Ishraq, M.A.R., Roy, S., A comparative neutronic analysis of U–Th fuels as potential alternatives to traditional UO2 fuel for enhance d performance and safety in the ACP-100 SMR., Int. J. Adv. Nucl. React. Des. Technol. 6 (2024), 177–184.

[7] JANIS (Java-based Nuclear Data Information System).


THANK YOU
Containment Structure
Pressurizer
Steam Generator
Control Rods
Reactor Vessel
Turbine
Generator
Condenser

2.METHODOLOGY
2.4.3 MOX fuel isotope composition for cutback

Fuel assembly types with cutback regions: B_0C, B_1C, B_2C, B_3C, C_0C, C_1C, C_2C, C_3C.

All cutback regions have the same enrichments.

In UO_2 fuel the enrichment of ^{235}U is kept 2 wt% in all zones, and in MOX fuel, the weight fractions are kept as following for all FAs and presented in Table 4:

Table 4. MOX fuel isotope composition for cutback

Enrichment	^{235}U (wt%)	^{238}U (wt%)	^{16}O (wt%)	^{232}Th (wt%)
Cutback	2.95	0.74	12.11	84.20

3. RESULTS
3.4 MTC and FTC parameters

Slide 16 — Comparison of FTC

•Primary mechanism: Fuel-temperature increases broaden resonance absorption peaks through the Doppler effect, changing neutron absorption and core reactivity.

•Fuel-composition effect: Different fertile-isotope inventories and resonance characteristics influence the magnitude of Doppler feedback.

•MOX interpretation: The more negative FTC indicates stronger negative fuel-temperature feedback in the calculated MOX core.

The neutron spectrum is the distribution of neutrons by energy.

•Primary mechanism: Moderator-density reduction changes neutron moderation and the neutron energy spectrum.

•Fuel-composition effect: Differences in 233U, 235U, 232 TH, 238u, reaction rates affect the resulting reactivity response.

Calculated conditions:

- Power level: 100% rated power,
- CBC: Determined using automatic critical boron search
- Xenon condition: equilibrium xenon, with $k_{eff} = 1.0$.

Comparison of MTC

•Primary mechanism: Moderator heating reduces water density, weakens neutron moderation, and changes the neutron energy spectrum.

•Additional factor: Soluble-boron concentration affects MTC when boron is present; its influence depends on the calculation conditions.

•MOX interpretation: Different isotope inventories and energy-dependent reaction cross sections may contribute to the non-monotonic MTC trend.

Primary mechanism: Doppler broadening of resonance absorption as fuel temperature increases.

•Fuel-composition effect: Differences in 232, 238 resonance absorption, isotope inventories, and neutron flux influence the magnitude of Doppler feedback.

•Calculated result: MOX exhibits more negative FTC than UO_2 throughout the evaluated cycle.

3. RESULTS
3.4.2 MTC and FTC parameters

Table 7 summarizes the calculated FTC and MTC values at three representative burnup points for each fuel.

Table 7. Comparison of FTC and MTC values.

Fuel	Burnup (GWd/MTU)	FTC (pcm/K)	MTC (pcm/K)
UO_2	0	−2.02	−15.92
	8.57	−2.13	−22.31
	17.13	−2.52	−53.20
MOX	0	−2.47	−18.43
	11.31	−2.62	−22.01
	22.61	−2.85	−39.45

This trend is consistent with the reduction in moderator density, which decreases neutron moderation, and the depletion of soluble boron, which weakens the positive reactivity contribution associated with boron dilution.

MOX fuel's different fuel composition changes the balance between neutron moderation, resonance absorption, and fission. During irradiation, 235U depletion and the conversion of 232Th into fissile 233U alter the isotopic composition and neutron spectrum. Together with changes in soluble boron and the depletion of gadolinium burnable absorbers, these effects may account for the temporary weakening of negative MTC during the middle of the cycle

3. RESULTS
3.5Microscopic cross sections

The microscopic fission and capture cross sections were generated in JANIS platform. [2]. The fission cross-sections compare ^{233}U and ^{235}U isotopes' microscopic cross sections and show fis sile-inventory effects. Although U-233 has a little lower cross sections in thermal region, it has a strong, isolated resonance near ~1.8 eV that gives it a distinctly higher fission cross section than U-235.

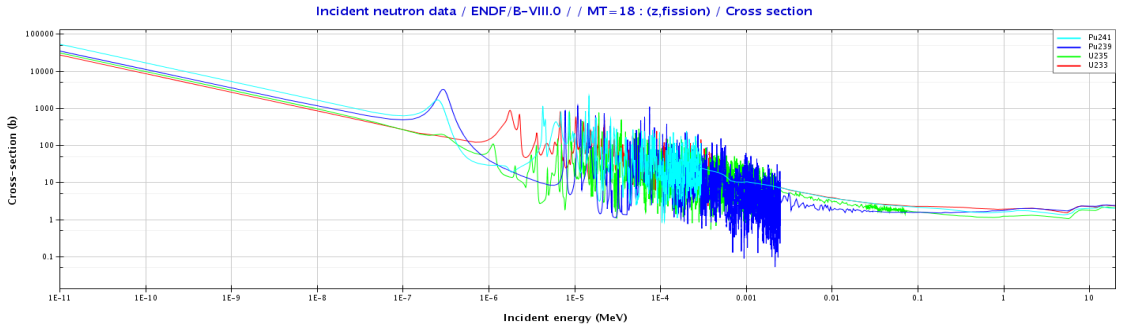


Fig. 10. Microscopic fission cross sections of fissile isotopes.

^{240}Pu and ^{242}Pu are the strongest isotopes in the resonance region, but their atom densities are small in my fuel, so they matter only after Pu has built up. Resonance integral for ^{238}U is about 275 b against about 85 b for ^{232}Th. UO_2 also has the ^{240}Pu resonance at 1.06 eV, which feeds ^{241}Pu production as burnup increases. Th-232's thermal capture cross section sits systematically above U-238 which means more absorber "mass" to Doppler-broaden per atom. Both isotopes exhibit energy-dependent capture resonances, which are important for neutron absorption and fertile-to-fissile conversion.

FTC is essentially a Doppler-broadening effect on the resonance capture cross section of the fertile absorber

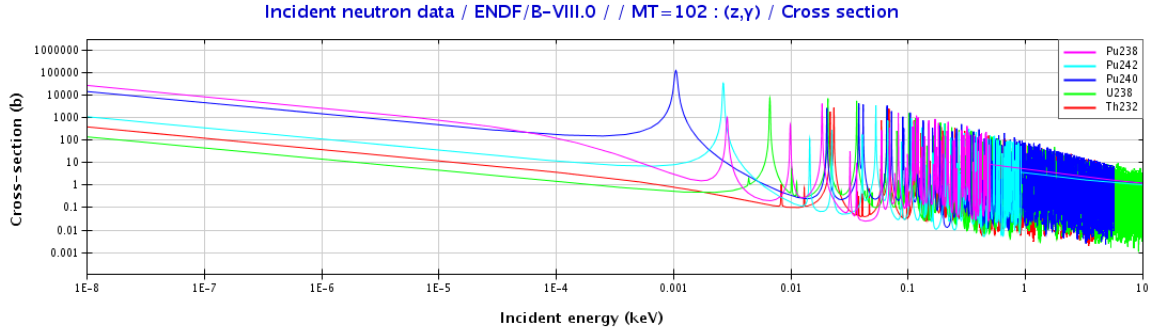


Fig. 11. Microscopic capture cross sections of fertile isotopes.

Fast flux

At constant reactor power, the neutron flux depends on the fission rate, energy released per fission, neutron production, and the fuel's energy-dependent reaction rates.

As irradiation progresses, fissile isotopes deplete and new fissile nuclides build up, changing the neutron balance and flux distribution. Boron and burnable-absorber depletion can also affect the evolving spectrum.

How do burnup effects change the flux ratio?

- Soluble-boron reduction: Less neutron absorption, mainly in the thermal-energy range, can allow more thermal neutrons to survive.
- Gadolinium depletion: Reduces strong thermal-neutron absorption, potentially increasing thermal flux relative to fast flux.
- Fuel-isotope evolution: Changes in fission and capture rates alter neutron production, absorption, and the energy distribution of neutrons.